Quasi-TEM Analysis of "Slow-Wave" Mode Propagation on Coplanar Microstructure MIS Transmission Lines

YOUNG RACK KWON, VINCENT M. HIETALA, STUDENT MEMBER, IEEE, AND KEITH S. CHAMPLIN, MEMBER, IEEE

***Abstract*—We present a simple quasi-TEM analysis of "slow-wave" mode propagation on micron-size coplanar MIS transmission lines on heavily doped semiconductors and compare theoretical results with measurements on four such structures at frequencies from 1.0 to 12.4 GHz. Excellent agreement is found, which shows that the "slow-wave" mode propagating on these transmission lines is, in fact, a quasi-TEM mode. Relatively low-loss propagation along with significant wavelength reduction is observed. Conduction losses of the metal, which have been tacitly ignored in previously published "full-wave" treatments of "slow-wave" mode propagation, are included in the theory and are shown to dominate the attenuation at frequencies below 25 GHz and to still be significant at frequencies up to at least 100 GHz.**

I. Introduction

COPLANAR metal–insulator–semiconductor (MIS) transmission lines on true (i.e., not semi-insulating) semiconductor substrates have applications in both monolithic microwave integrated circuits (MMIC's) and very high speed digital integrated circuits (VHSDIC's). Such structures have been studied experimentally by Hasegawa and coworkers, who reported measurements of "slowing factor" and characteristic impedance magnitude [1] and of attenuation coefficient [2] as functions of frequency over the range from 700 MHz to 4 GHz. Their papers refer to a quasi-TEM analysis of their coplanar MIS structure. However, their analysis does not include the effects of losses; nor does it explain the observed frequency dependence of the experimentally determined quantities.

More extensive numerical analyses of coplanar MIS transmission lines on semiconductors have been described by other investigators [3]–[8]. These so-called full-wave treatments have been based upon either the classical mode-matching (MM) method [3]–[6], the spectral-domain analysis (SDA) method [4], [7], [8], or the finite-element method (FEM) [8]. Although such computational techniques have generally included semiconductor losses, they have tacitly assumed perfect metallic conductors. Accordingly, metal losses have been systematically ignored.

Manuscript received November 8, 1986; revised January 24, 1987. This work was supported in part by the U.S. Army Research Office and the National Science Foundation under Grant ECS-83-16246 and by a grant from the Microelectronic and Information Sciences Center of the University of Minnesota.

The authors are with the Electrical Engineering Department, University of Minnesota, Minneapolis, MN 55455.

IEEE Log Number 8714119.

This paper presents a simple quasi-TEM analysis of coplanar microstructure MIS transmission lines on heavily doped semiconductors propagating the "slow-wave" mode. Preliminary measurements on such a structure have recently been reported [9]. The theory includes metal losses as well as semiconductor losses and employs an equivalent circuit model that is similar to those used by others to analyze Schottky and MIS microstrip transmission lines [10]–[12] and Schottky coplanar transmission lines [13], [14]. Quantities derived from this quasi-TEM theory are compared with quantities measured in the range from 1.0 to 12.4 GHz using four coplanar MIS microstructure transmission lines fabricated on N^+ silicon. Excellent agreement between theory and experiment is observed. Such close agreement corroborates the assumption that the "slow-wave" mode propagating on these microstructure MIS transmission lines is, in fact, a quasi-TEM mode and can therefore be treated by fairly elementary techniques.

Relatively low-loss microwave propagation along with significant wavelength reduction is predicted by the theory and confirmed by the experiments. Such properties suggest that coplanar microstructure MIS transmission lines on heavily doped semiconductors may be useful as transmission media for fabricating distributed components of MMIC's. The theory shows that metal losses of the experimental transmission lines are very significant at frequencies below 100 GHz and, in fact, constitute the dominant loss mechanism at frequencies below about 25 GHz. Thus, the previously published "full-wave" analysis treatments [3]–[8], because of their systematic omission of metal losses, are deemed inadequate for accurate analysis of these microstructure transmission lines.

II. Experimental Results

The geometry of the experimental microstructure transmission lines is shown in Fig. 1. These structures employed coplanar aluminum strips separated from an N^+ silicon substrate by a thin layer of SiO_2. The SiO_2 was grown on antimony-doped, N^+ silicon (80 $(\Omega\cdot\text{cm})^{-1}$, $N_d \approx 3\times10^{18}$ cm^{-3}) by wet oxidation at 1000°C. The center conductor and ground planes were fabricated by evaporating aluminum onto the SiO_2 and defining the conducting structure using standard photolithographic and etching

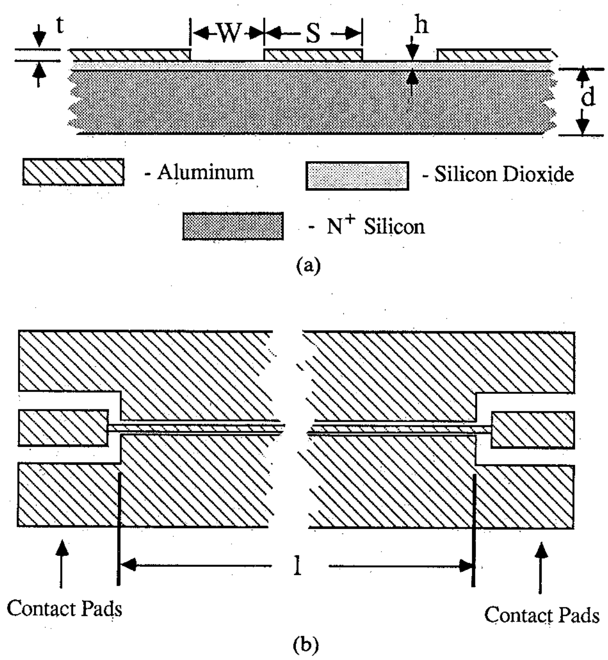

Fig. 1. (a) Cross-sectional view and (b) plan view of micron-sized coplanar MIS transmission line.

TABLE I

DIMENSIONS (S, W, h) AND CAPACITANCE SCALING FACTOR (K) OF THE EXPERIMENTAL LINES

Line	S	W	h	K
1	4.2	6.0	0.53	1.3
2	4.2	14.0	0.53	1.3
3	8.7	9.5	0.28	1.1
4	4.7	13.5	0.28	1.2

All dimensions are in micrometers.

techniques. The resulting line dimensions (defined in Fig. 1) are summarized in Table I. For all four transmission lines, the wafer thickness (d) was 530 μm, the length (l) was 2500 μm, and the metal thickness (t) was 1 μm.

S-parameter measurements were performed over the range from 1.0 GHz to 12.4 GHz with a computer-assisted HP 8410B test set employing a 12-term error-correction procedure. Contacts to the lines were made with a pair of Cascade Microtech[1] microwave probes which provided rapid, reproducible measurements free of packaging considerations. The complex characteristic impedance and complex propagation coefficient were derived from the measured S parameters after first subtracting the capacitive effects of the contact pads.

As seen in Fig. 2, the attenuation of each of the lines is quite small. The maximum observed attenuation, approximately 2 dB/mm (line 3) at 12.4 GHz, is, to the best of our knowledge, considerably less than any microwave attenuation value reported by others for transmission lines on room-temperature silicon. Fig. 3 displays the real and imaginary parts of the characteristic impedance as functions of frequency. One sees that all four lines have characteristic impedances which are nearly real, relatively independent of frequency, and of the order of the 50-Ω impedance commonly used in microwave circuits. Line 2, in particular, has a characteristic impedance of approximately 44 Ω.

[1] Cascade Microtech, Inc., P.O. Box 1589, Beaverton, OR 97075-1589.

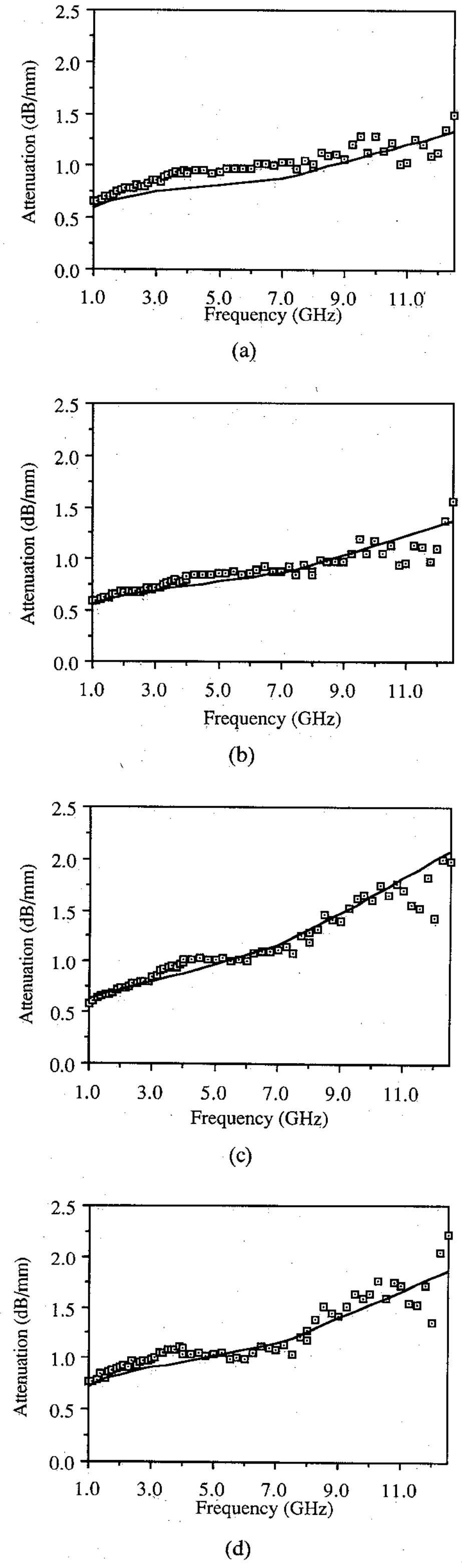

Fig. 2. Attenuation versus frequency. (a) Line 1. (b) Line 2. (c) Line 3. (d) Line 4. Solid lines are theoretical. Symbols are measured values.

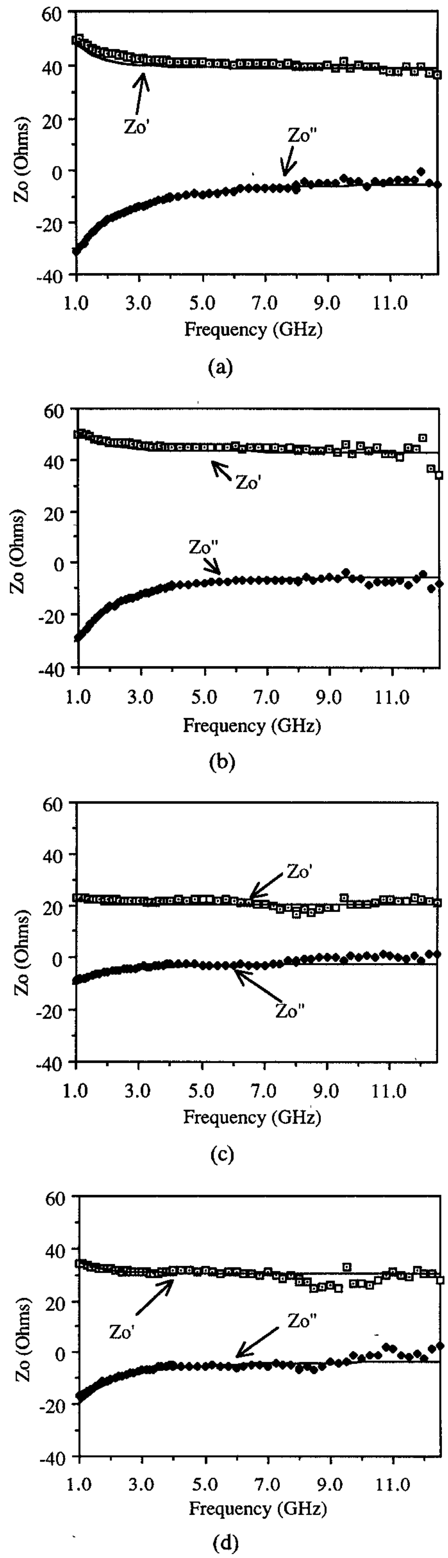

Fig. 3. Complex characteristic impedance versus frequency. (a) Line 1. (b) Line 2. (c) Line 3. (d) Line 4. Solid lines are theoretical. Symbols are measured values.

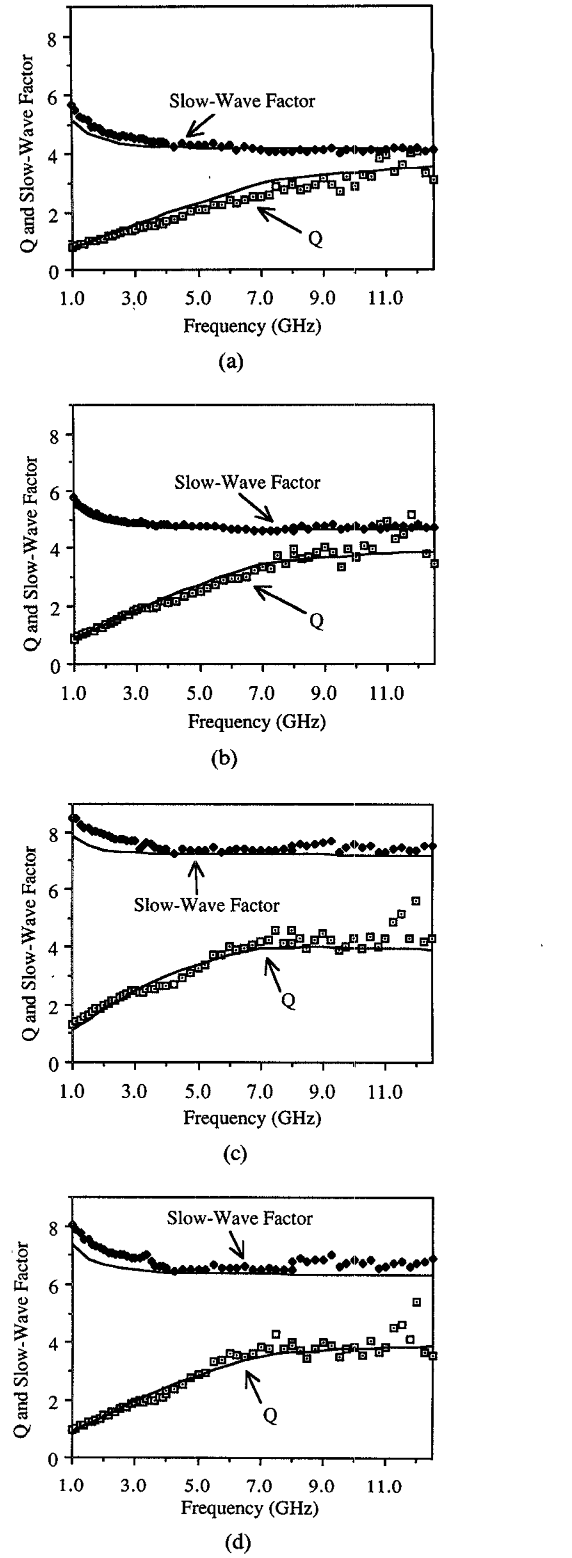

Fig. 4. Quality and slow-wave factors versus frequency. (a) Line 1. (b) Line 2. (c) Line 3. (d) Line 4. Solid lines are theoretical. Symbols are measured values.

Fig. 4 shows the "slowing factors" λ_0/λ_g as functions of frequency and displays values greater than 4 with very little dispersion occurring over the full range of measurement. The largest slowing factor observed, 7.5 (line 3), corresponds to an effective dielectric constant 56.3—a value much larger than the dielectric constant of either Si or SiO_2. This fact, along with the relatively low loss, confirms operation in a "slow-wave" mode. Additional proof of slow-wave mode propagation is given below in Section IV. Fig. 4 also displays the quality factor Q versus frequency. One sees that the four quality factors increase with frequency and reach values ranging from 3.6 to 4.3 at

12.4 GHz. These values may be compared with quality factors of approximately 1.6 at 1 GHz and 0.9 at 2 GHz obtained by Hasegawa and coworkers [1], [2] using a much larger MIS coplanar structure on GaAs.

III. Quasi-TEM Analysis

The validity of our quasi-TEM analysis is based upon the assumption that transverse dimensions are so small that transverse fields are, to first-order, quasi-static. Because of the low impedance of the N^+ semiconductor, most of the electrical energy is thereby confined to the lossless insulating layer immediately below the center conductor [13]. However, the magnetic field freely penetrates the N^+ substrate because the dimensions of the line are so small that the quasi-static range of magnetic field is much less than the semiconductor's skin depth ($\delta_S \approx 56$ μm at 10.0 GHz). Thus, since the skin effect is unimportant and the semiconductor is a nonmagnetic material, to first-order the magnetic field does not "see" the N^+ layer at all. Accordingly, the magnetic field distribution is nearly that of normal coplanar waveguide (CPW) on an insulating substrate [13]. This separation of electric and magnetic energies results in slow-wave mode propagation.

For quasi-TEM propagation, one can introduce an inductance per unit length, L, which can be expressed as

$$L = \frac{1}{c^2 C'} \tag{1}$$

where c is the free-space phase velocity and C' is the capacitance per unit length of an equivalent air-filled transmission line. Since the magnetic field of the present structure is nearly that of normal CPW, C' can be determined by conformal mapping. This leads to [15]

$$L = \frac{1}{4c^2 \epsilon_0 F} \tag{2}$$

where ϵ_0 is the permittivity of free space and F is a geometrical factor which can be approximated by [15]

$$F = \begin{cases} \dfrac{\ln\left(\dfrac{2(1+\sqrt{k})}{(1-\sqrt{k})}\right)}{\pi} & \text{for } 0.707 \leqslant k \leqslant 1 \\ \dfrac{\pi}{\ln\left(\dfrac{2(1+\sqrt{k'})}{(1-\sqrt{k'})}\right)} & \text{for } 0 \leqslant k \leqslant 0.707 \end{cases} \tag{3}$$

in which

$$k = \frac{S}{S+2W} \tag{4}$$

and

$$k' = \sqrt{1-k^2}. \tag{5}$$

The longitudinal inductance L is shown in the equivalent circuit of Fig. 5.

The metal conductive losses are introduced as a correction represented by the resistance R_m in series with L in Fig. 5. This longitudinal loss resistance, expressed in ohms per unit length, is approximated in our simple model by the effective resistance of the center conductor:

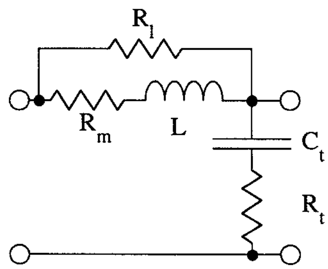

Fig. 5. "Slow-wave" mode equivalent circuit of coplanar microstructure MIS transmission line used in quasi-TEM analysis.

$$R_m = \begin{cases} \dfrac{1}{\sigma_m t S} & \text{for } t \leqslant \delta_m \\ \dfrac{1}{\sigma_m \delta_m S} & \text{for } t \geqslant \delta_m \end{cases} \tag{6}$$

where σ_m and δ_m are the conductivity and skin depth, respectively, of the aluminum. Since current densities in the ground planes are much less than in the center conductor, the ground plane contribution to R_m is ignored.

Longitudinal current, which parallel the current of the center conductor, flows in the N^+ semiconductor immediately under the center conductor and also contributes to loss [11], [12]. This current is essentially a correction to the assumption of no interaction between the magnetic field and the N^+ semiconductor. Losses associated with longitudinal current in the semiconductor are represented by R_L in Fig. 5. Since the longitudinal semiconductor current flows in addition to the longitudinal current in the metal, a parallel connection was employed rather than the series connection of Seguinot *et al.* [13], [14]. In our model, R_L is given by

$$R_L = \frac{1}{\sigma_S \delta_S S} \tag{7}$$

where σ_S and δ_S are the conductivity and skin depth, respectively, of the N^+ semiconductor. Equation (7) is based upon the assumption that the longitudinal E field under the center conductor decays exponentially in the vertical direction with decay constant δ_S. Note that the assumption of small dimensions applies only to the transverse dimensions and does not preclude skin effect behavior of the longitudinal electric field.

Energy storage and loss associated with the transverse electric field and current are represented by the transverse capacitance C_t and transverse resistance R_t, respectively, in Fig. 5. Since electric energy storage is largely confined to the dielectric layer under the center conductor, the transverse capacitance per unit length is approximated by

$$C_t = \frac{S \epsilon_i \epsilon_0 K}{h} \tag{8}$$

where ϵ_i is the dielectric constant of SiO_2 and K is a geometric factor slightly larger than unity introduced to account for field fringing. The K values used for each transmission line are given in Table I. These values were found by using finite-difference calculations to determine the exact static capacitance of each line. Results are not critically dependent on K values, however. Maximum errors in Z_0 and γ of only about 10 percent will result from simply letting $K = 1$.

For the N^+ semiconductor, $\sigma_S \gg \omega\epsilon_S\epsilon_0$, where ϵ_S is the relative dielectric constant of silicon. Accordingly, transverse current flow is predominantly resistive and is represented by R_t in series with C_t in Fig. 5. In the present model, this transverse resistance is approximated by

$$R_t = \frac{1}{2\sigma_S F} \tag{9}$$

where F is the geometric factor defined in (3). The derivation of (9) is based upon the analogy between the transverse resistance of the present structure and the inverse transverse capacitance of normal CPW.

In principle, there should also be a transverse capacitance through the air [13], [14]. However the susceptance of this capacitance is very small compared with the susceptance of C_t and R_t in series and is ignored in our model.

For a particular transmission line implementation, the circuit elements of Fig. 5 were evaluated as functions of frequency using (2)–(9). The complex propagation coefficient γ and complex characteristic impedance Z_0 were then determined from

$$\gamma = \alpha + j\beta = \sqrt{ZY} \tag{10}$$

$$Z_0 = Z_0' + jZ_0'' = \sqrt{\frac{Z}{Y}} \tag{11}$$

where

$$Z = \frac{1}{\dfrac{1}{R_L} + \dfrac{1}{j\omega L + R_m}} \tag{12}$$

$$Y = \frac{1}{R_t + \dfrac{1}{j\omega C_t}}. \tag{13}$$

Finally, the quality factor Q and "slowing factor" (λ_0/λ_g) were determined from

$$Q = \frac{\beta}{2\alpha} \tag{14}$$

and

$$\frac{\lambda_0}{\lambda_g} = \frac{\beta}{\omega\sqrt{\mu_0\epsilon_0}}. \tag{15}$$

IV. Range of Validity

The quasi-TEM analysis described above assumes quasi-static fields having a depth of penetration into the N^+ semiconductor that is small compared with the semiconductor skin depth. From the results of Davis, Williams, and Celestini [16], we conservatively estimate this quasi-static field range to be $(S/2 + W)$. For our quasi-TEM model to apply, the frequency f must therefore be small compared with the frequency f_1 for which the skin depth equals $(S/2 + W)$:

$$f_1 = \frac{1}{\pi\sigma_S\mu_0(S/2 + W)^2}. \tag{16}$$

In addition, (9) assumes that $\omega\epsilon_S\epsilon_0 \ll \sigma_S$. This implies that the frequency f is small compared with the dielectric relaxation frequency f_2, defined to be

$$f_2 = \frac{\sigma_S}{2\pi\epsilon_0\epsilon_S}. \tag{17}$$

We conclude that the quasi-TEM mode analysis presented above is only valid at frequencies which satisfy both $f \ll f_1$ and $f \ll f_2$.

The two frequencies defined in (16) and (17) can also be used to differentiate between three different modes of propagation [10]. For $f_2 < f < f_1$, transverse electric and magnetic fields both freely penetrate the semiconductor substrate and propagation of the "dielectric quasi-TEM mode" occurs. For $f_1 < f < f_2$, the mode of propagation is the "skin-effect mode" in which neither field penetrates into the semiconductor substrate. Finally, for $f \ll f_1$ and $f \ll f_2$, the mode of propagation will be a "slow-wave" mode. In this region, the magnetic field freely penetrates the semiconductor substrate while the electric field does not. These last conditions are also those required for the quasi-TEM model presented above to apply. Using worst-case parameters for the four transmission lines under consideration, $f_1 = 120$ GHz and $f_2 = 12000$ GHz. Thus, by comparing f_1 and f_2 to the maximum measurement frequency of 12.4 GHz, one sees that all four lines easily meet the criteria for "slow-wave" mode propagation and for validity of the above quasi-TEM analysis technique.

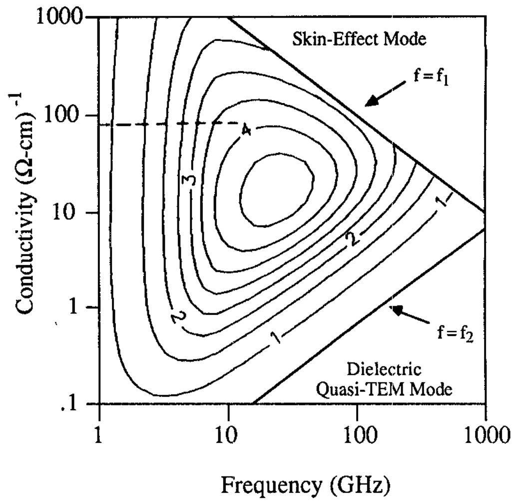

Fig. 6. Contours of constant Q in the "slow-wave" mode region for transmission line 2. Dashed line corresponds to experiment.

Fig. 6 shows a calculated family of contours of constant Q in the conductivity–frequency plane for the geometry of transmission line 2. The boundaries of the quasi-TEM "slow-wave" mode region that occur at $f = f_1$ and $f = f_2$ are shown in this figure. The dashed line on the left identifies the semiconductor conductivity of transmission line 2 and corresponds to actual experimental conditions. One sees that the experiment falls well within the realm of quasi-TEM "slow-wave" mode propagation throughout the entire experimental frequency range. In addition, one notes from Fig. 6 that the conductivity of transmission line 2 is somewhat larger than the conductivity that would be desired to obtain maximum Q.

V. Discussion

The quasi-TEM analysis technique described above was used to calculate the theoretical curves plotted in Figs. 2–4. Excellent agreement between theory and experiment is noted for all four lines over the full frequency range from 1.0 to 12.4 GHz. Such close agreement is typical of results we have obtained on other lines fabricated on similar substrates but having center conductor widths ranging from $S = 4.2$ μm to $S = 15$ μm and gap widths ranging from $W = 6$ μm to $W = 21$ μm. This apparent validity of the simple quasi-TEM theory is believed to be due in large part to the very small cross-sectional dimensions, which ensure that transverse fields are essentially quasi-static. The excellent agreement corroborates the assumptions that the "slow-wave" mode propagating on these microstructure MIS transmission lines is, in fact, a quasi-TEM mode and is therefore amenable to analysis by elementary techniques.

The relative importance of each of the three loss mechanisms can be theoretically investigated by using the quasi-TEM theory to separately calculate the attenuation with only one of the three resistive elements included in the equivalent circuit. When this is done for each of the three resistive elements, it is found that the sum of the three partial attenuations equals the total attenuation, with all three elements included, to within a 1-percent error. Thus, the ratio of each partial attenuation to the total attenuation accurately reflects the relative contribution of each individual loss mechanism to the total attenuation of the line.

Fig. 7 shows a plot of the relative contribution of each individual loss mechanism to the total attenuation of transmission line 2. One sees that the metal loss contribution decreases with increasing frequency but is dominant at frequencies below about 25 GHz. Even at frequencies as high as 100 GHz, metal losses still account for nearly 20 percent of the total attenuation. Clearly, gross inaccuracies would result from neglecting the metal losses. The transverse and longitudinal semiconductor losses are both seen to increase with frequency. However, the transverse-loss component is very small. For example, one sees from Fig. 7 that R_t is responsible for less than 10 percent of the total attenuation at frequencies below 100 GHz.

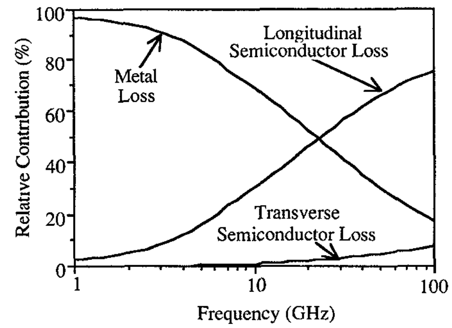

Fig. 7. Contribution of each loss mechanism to the total attenuation of transmission line 2.

VI. Conclusions

The simple quasi-TEM analysis technique presented above is seen to provide excellent agreement with measurements of micron-size coplanar MIS transmission lines on heavily doped silicon propagating the "slow-wave" mode. Such close agreement is attributed to the very small cross-sectional dimensions of the transmission lines, which ensure that transverse fields are essentially quasi-static. Besides its apparent validity in the "slow-wave" mode region, the quasi-TEM approach is quite easy to use and provides useful insight into "slow-wave" propagation and the roles played by the different loss mechanisms.

In contrast with previously published "full-wave" analysis treatments [3]–[8], the present quasi-TEM analysis takes metal losses into consideration. This is important since metal losses are found to actually dominate the attenuation at frequencies below 25 GHz and to still be significant at frequencies up to at least 100 GHz. Accordingly, the earlier full-wave analysis treatments are deemed inadequate for accurate analysis of these microstructure transmission lines.

Micron-size coplanar MIS transmission lines on heavily doped semiconductors possess a number of properties that are desirable for MMIC's. They are easy to analyze, easy to fabricate, have very confined fields, exhibit relatively low loss, have reasonably large slowing factors, have convenient values of characteristic impedance, and demonstrate very little dispersion over a broad range of microwave frequencies. In addition, they can be fabricated on thick, robust, substrates and do not require "vias" for connections to the ground plane. These properties suggest that such lines may be useful as transmission media for fabricating distributed components in MMIC's. By optimizing dimensions and materials, it should be possible to further reduce attenuation, significantly increase Q, and extend the useful range of operation well into the millimeter-wave spectrum.

References

[1] H. Hasegawa and H. Okizaki, "M.I.S. and Schottky slow-wave coplanar striplines on GaAs substrates," *Electron. Lett.*, vol. 13, no. 22, pp. 663–664, Oct. 1977.

[2] S. Seki and H. Hasegawa, "Cross-tie slow-wave coplanar waveguide on semi-insulating GaAs substrates," *Electron. Lett.*, vol. 17, no. 25, pp. 940–941, Dec. 1981.

[3] Y. Fukuoka and T. Itoh, "Analysis of slow-wave phenomena in coplanar waveguide on a semiconductor substrate," *Electron. Lett.*, vol. 18, no. 14, pp. 589–590, July 1982.
[4] Y. Fukuoka, Y. Shih, and T. Itoh, "Analysis of slow-wave coplanar waveguide for monolithic integrated circuits," *IEEE Trans. Microwave Theory Tech.*, vol. MTT-31, pp. 567–573, July 1983.
[5] R. Sorrentino and G. Leuzzi, "Full-wave analysis of integrated transmission lines on layered lossy media," *Electron. Lett.*, vol. 18, no. 14, pp. 607–608, July 1982.
[6] R. Sorrentino, G. Leuzzi, and A. Silbermann, "Characteristics of metal–insulator–semiconductor coplanar waveguides for monolithic microwave circuits," *IEEE Trans. Microwave Theory Tech.*, vol. MTT-32, pp. 410–415, Apr. 1984.
[7] Y. C. Shih and T. Itoh, "Analysis of printed transmission lines for monolithic integrated circuits," *Electron Lett.*, vol. 18, no. 14, pp. 585–586, July 1982.
[8] M. Aubourg *et al.* "Analysis of M.I.S. or Schottky contact coplanar lines using the F.E.M. and the S.D.A.," in *IEEE MTT-S Int. Microwave Symp. Dig.*, 1983, pp. 396–398.
[9] V. M. Hietala, Y. R. Kwon, and K. S. Champlin, "Low-loss slow-wave propagation along a microstructure transmission line on a silicon surface," *Electron. Lett.*, vol. 22, no. 14, pp. 755–756, July 1986.
[10] H. Hasegawa, M. Furukawa, and H. Yanai, "Properties of microstrip line on Si–SiO_2 system," *IEEE Trans. Microwave Theory Tech.*, vol. MTT-19, pp. 869–881, Nov. 1971.
[11] D. Jäger, W. Rabus, and W. Eichkoff, "Bias-dependent small-signal parameters of Schottky contact microstrip lines," *Solid-State Electron.*, vol. 17, pp. 777–783, 1974.
[12] D. Jäger, "Slow-wave propagation along variable Schottky-contact microstrip line," *IEEE Trans. Microwave Theory Tech.*, vol. MTT-24, pp. 566–573, Sept. 1976.
[13] C. Seguinot, P. Kennis, and P. Pribetich, "Desktop computer appraisal of potential slow-wave propagation characteristics for Schottky coplanar lines," *Electron. Lett.*, vol. 19, no. 25, pp. 1065–1067, Dec. 1983.
[14] C. Seguinot, P. Kennis, P. Pribetich, and J. F. Legier, "Analytical model of Schottky contact coplanar line," in *Proc. 14th European Microwave Conf.* (Liege), 1984, pp. 160–165.
[15] K. C. Gupta, R. Garg, and I. J. Bahl, *Microstrip Lines and Slotlines.* Dedham, MA: Artech House, 1979, p. 261 and 275.
[16] M. E. Davis, E. W. Williams, and A. C. Celestini, "Finite-boundary corrections to the coplanar waveguide analysis," *IEEE Trans. Microwave Theory Tech.*, vol. MTT-21, pp. 594–596, Sept. 1973.

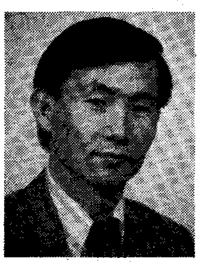

Young Rack Kwon received the B.S. degree from the Republic of Korea Air Force Academy in 1974. He then transferred to the Seoul National University, where he received the B.S. degree in electronic engineering in 1977 and the M.S. degree in electronic engineering in 1980.

In 1977, he became a member of the Korea Air Force Academy faculty board, a position that he still holds. Since 1983, he has been working toward the Ph.D. degree in electrical engineering at the University of Minnesota under a Korean Air Force Scholarship. His interests are in monolithic microwave integrated circuits and devices.

Vincent M. Hietala (S'85) was born in Virginia, MN, on September 18, 1961. He received the B.E.E. degree (with high distinction) in 1983 and the M.S.E.E. degree in 1987, both from the University of Minnesota.

In 1983, he received an MEIS Doctoral Fellowship from the Microelectronic and Information Sciences Center at the University of Minnesota. In 1986, he was awarded a General Electric Foundation Fellowship. He also received the 1986 Rosemount Instrumentation Award for work in microwave measurements.

Mr. Hietala is currently working toward the Ph.D. degree in electrical engineering at the University of Minnesota. He is a Research Assistant and is doing research in microwave and semiconductor device theory.

Keith S. Champlin (S'56–M59) has been a member of the Electrical Engineering faculty of the University of Minnesota since 1958 and has held a full professorship in that department since 1967. In addition, he holds an adjunct appointment in the Physics Department of the University of Minnesota and has served as Visiting Professor at the Laboratoire de Physique, Ecole Normale Superiour in Paris, France, working under Dr. P. Aigrain. At the University of Minnesota, Dr. Champlin has been twice honored by receiving the Institute of Technology's "Distinguished Teaching Award" as well as the IT Student Board's "Outstanding Teacher Award."

After having served as a Master Sergeant with the U.S. Army Signal Corps in 1951 and 1952, Dr. Champlin completed his undergraduate studies and entered graduate school at the University of Minnesota. As a graduate student he studied noise in semiconductor materials and devices under Prof. A. Van der Ziel. His thesis research dealt with noise in silicon pn junctions, particularly in junctions undergoing avalanche breakdown. Since 1960, Dr. Champlin's research effort has been primarily concerned with investigations of semiconductor material properties and semiconductor devices at microwave and millimeter-wave frequencies. At the present time, Dr. Champlin is directing an active group engaged in research on linear and nonlinear distributed devices having applications to monolithic microwave and millimeter-wave integrated circuits. He is also consulting with industry in these areas.

Dr. Champlin has authored approximately 65 publications in the fields of semiconductors and microwaves. He has six patents issued and one patent pending in the United States and 17 patents issued in foreign countries. Several of his inventions have been commercially successful and are presently being manufactured. He holds a Private Pilot's License, a First Class Commercial Radiotelephone License, and an Extra Class Amateur Radio License. Dr. Champlin is a member of the American Physical Society, the American Association for the Advancement of Science, Eta Kappa Nu, Tau Beta Pi, Gamma Alpha, and Sigma Xi.